Discrete minimal surfaces of Koebe type

Alexander I. Bobenko, Ulrike Bücking, Stefan Sechelmann

March 5, 2018

1 Introduction

Minimal surfaces have been studied for a long time, but still contain unsolved aspects. Stimulated by the relevance for computer graphic and visualization, there is actually an increasing interest to find suitable discrete analogs for known geometric notions and shapes like minimal surfaces. Usually, one can suggest various discretizations which have quite different properties. See [13, 35, 15, 24, 16, 6, 21] for a choice of examples from the huge variety of different approaches for discrete minimal surfaces. We consider this class of surfaces in the context of discrete differential geometry. The goal of this theory is to find a discretization which inherits as many essential properties of the smooth theory as possible.

Our approach is based on the discretization of parametrized surfaces which lead to quadrilateral meshes. In particular, we choose a parametrization where the second fundamental form is diagonal. Such *conjugate nets* exist (locally) for general surfaces in $\mathbb{R}^3$ and lead to discrete parametrized surfaces built from planar quadrilateral faces, which are particular *polyhedral surfaces*. In addition to the discrete surface we consider a line congruence at the vertices which can be interpreted as a discrete Gauss map. This easily leads to parallel offset meshes, see Figure 3 below. Comparing the areas of two such parallel planar quadrilaterals can then be used to define discrete mean and Gaussian curvature analogously as in the smooth case. This approach leads to a simple notion of discrete minimal surfaces which contains several known definitions as special cases.

We especially focus on discrete minimal surfaces whose discrete Gauss map is given by a Koebe polyhedron, i.e. a polyhedral surface with edges tangent to the unit sphere. This case is closely connected to the theory of S-isothermic discrete minimal surfaces as studied in [1]. We remind the construction scheme which, in particular, allows to build an analogon for (a finite part of) any given smooth minimal surface.

S-isothermic discrete minimal surfaces can be constructed using suitable orthogonal circle patterns. These are configurations of circles for a given planar graph G such that to each vertex of G there corresponds a circle. If two vertices are connected by an edge in G then the corresponding circles intersect orthogonally. The circles corresponding to the vertices of a face of G intersect in one point. Furthermore, for any circle corresponding to an interior vertex the disks filling the neighboring circles have mutually disjoint interiors. For the construction of such circle patterns we use a variational principle from [5, 34]. This has advantages for the explicit calculation of examples and has been used to create our various examples of Section 4.

An important connection to the smooth theory is demonstrated by the convergence of a large class of S-isothermic discrete minimal surfaces to their smooth analogons. The main ideas are explained in Section 5; for a detailed version and a proof see [10].

2 Discrete minimal surfaces

Every smooth immersed surface in $\mathbb{R}^3$ can (locally) be written as a parametrization, that is as a smooth mapping

$$\mathcal{F} : \mathbb{R}^2 \supset D \to \mathbb{R}^3, \quad (x, y) \mapsto \mathcal{F}(x, y),$$

such that in any point the partial derivatives $\partial_x \mathcal{F}$ and $\partial_y \mathcal{F}$ are linearly independent. We focus on special parametrizations where the second fundamental form is diagonal, that is $\partial_{xy} \mathcal{F} \in \operatorname{span}(\partial_x \mathcal{F}, \partial_y \mathcal{F})$, where ∂_{xy} denotes the mixed partial derivative. Such parametrizations are also called *conjugate nets*. This condition can be interpreted as the planarity of infinitesimal quadrilaterals with vertices $\mathcal{F}(x, y)$, $\mathcal{F}(x + \varepsilon, y)$, $\mathcal{F}(x + \varepsilon, y + \varepsilon)$, $\mathcal{F}(x, y + \varepsilon)$. As a discrete analog, it is therefore natural to consider discrete parametrized surfaces built from planar quadrilateral faces. The corresponding discrete parameter space will be a special cell decomposition.

Recall that a *cell decomposition of a two-dimensional manifold* possibly with boundary is a graph embedded in the manifold such that the complement of the graph is (topologically) a disjoint union of open disks. Thus, a cell decomposition decomposes a two-dimensional manifold into vertices, edges, and faces. The sets of vertices and edges will be denoted by V and E respectively. The cell decomposition is called *regular*, if it has no loops (edges with the same vertex on both ends), and if the boundary of a face contains an edge or vertex at most once. A regular cell decomposition is called *strongly regular* if two edges have at most one vertex in common at their boundaries, and if two faces have at most one edge or one vertex in common at their boundaries.

Definition 2.1. A strongly regular cell decomposition $\mathscr{D}$ of a two-dimensional oriented manifold possibly with boundary is called a *quad-graph*, if all 2-cells (faces) of $\mathscr{D}$ are embedded, carry the same orientation, and are quadrilaterals, that is there are exactly four edges incident to each face. See Figure 1 for an example.

A mapping $F : \mathscr{D} \to \mathbb{R}^3$ from a quad-graph $\mathscr{D}$ is called a *quadrilateral surface* if each face of $\mathscr{D}$ is mapped by F to a planar quadrilateral in $\mathbb{R}^3$, see Figure 2.

Given a smooth immersed surface $\mathcal{F} : \mathbb{R}^2 \supset D \to \mathbb{R}^3$ there exists in every point a normal direction, i.e. a line orthogonal to the surface. In fact, there is even (locally) a smooth map $\mathcal{N} : D \to \mathbb{S}^2$, called Gauss map, such that $\mathcal{N}(p)$ is orthogonal to the surface at $\mathcal{F}(p)$. As a discrete analogon of normals to a surface we introduce lines at the vertices building a line congruence:

Definition 2.2. Let $\mathbb{L}^3$ be the space of affine lines in $\mathbb{R}^3$ and denote by $\mathbb{L}^3(p)$ the subset of affine lines in $\mathbb{R}^3$ passing through the point $p \in \mathbb{R}^3$. A *line congruence* for a quadrilateral surface $F : \mathscr{D} \to \mathbb{R}^3$ is a mapping $\ell : V(\mathscr{D}) \to \mathbb{L}^3$ which assigns to every vertex $v \in V(\mathscr{D})$ an affine line $\ell(v) \in \mathbb{L}^3(F(v))$ such that for neighboring vertices v_i, v_j the corresponding lines $\ell(v_i)$ and $\ell(v_j)$ are coplanar, i.e. intersect or are parallel.

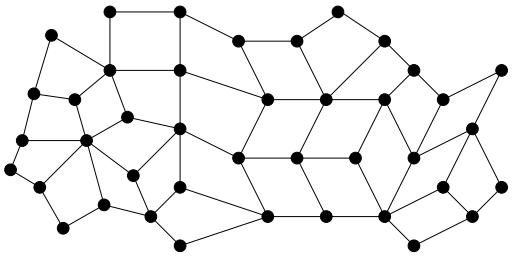

Figure 1: Example of a quad-graph

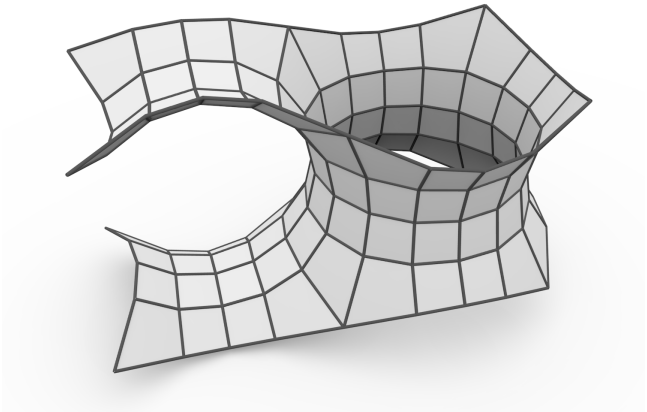

Figure 2: Example of a quadrilateral surface

Remark 2.3. Line congruences belong to projective geometry. Therefore, instead of affine lines in $\mathbb{L}^3$, it is natural to consider the space of lines in $\mathbb{RP}^3$.

Given a quadrilateral surface $F : \mathscr{D} \to \mathbb{R}^3$ with a line congruence ℓ note that for every edge $e = [v_1, v_2] \in E(\mathscr{D})$ joining the vertices v_1, v_2 the lines $\ell(v_1)$ and $\ell(v_2)$ and the edge of the surface $F([v_1, v_2])$ are coplanar. Therefore one can easily construct parallel surfaces to F, see Figure 3 (left).

Conversely, given two such parallel quadrilateral surfaces F_1 and F_2, we can easily obtain a line congruence by adding lines through corresponding points. Furthermore, the vectors joining the points corresponding to the same vertex v can be interpreted as a *generalized discrete Gauss map* $N(v) = F_2(v) - F_1(v)$. Now consider these vectors for one face of the quadrilateral surface F_1 and translate the vectors within that face such that they all start at one vertex, see Figure 3 (right). Their endpoints still lie in the corresponding plane of the parallel surface F_2. Thus moving all vectors $N(v)$ such that they all start at the origin we again obtain a quadrilateral surface $N : \mathscr{D} \to \mathbb{R}^3$ parallel to F_1 and F_2.

These reasonings show that for a given quadrilateral surface F we can identify a line congruence ℓ with a one parameter family λN for $\lambda \neq 0$ of associated generalized discrete Gauss maps by $\ell(v) = \{F(v) + \mu N(v) \ : \ \mu \in \mathbb{R}\}$ for every vertex v.

Definition 2.4. A quadrilateral surface $F : \mathscr{D} \to \mathbb{R}^3$ with a generalized discrete

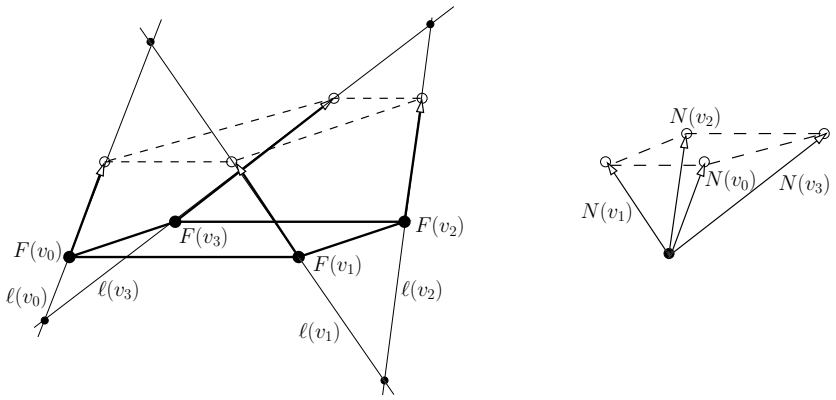

Figure 3: *Left:* Planar face of a quadrilateral surface F with line congruence ℓ and a corresponding parallel face (dashed lines), *Right:* Corresponding face of the associated generalized discrete Gauss map N

Gauss map $N : \mathscr{D} \to \mathbb{R}^3$, i.e. a parallel quadrilateral surface N, is called a *line congruence net* (F, N).

2.1 Discrete curvatures

Given a smooth surface $\mathcal{F}$ with its Gauss map $\mathcal{N}$, a parallel surface $\mathcal{F}_t$ can (locally) be defined by the formula $\mathcal{F}_t = \mathcal{F} + t\mathcal{N}$ for sufficiently small $t \in \mathbb{R}$. The classical *Steiner formula* states that the infinitesimal area of the parallel surface $\mathcal{F}_t$ is the quadratic polynomial

$$dA(\mathcal{F}_t) = (1 - 2tH + t^2K)dA(\mathcal{F}). \tag{1}$$

Here $dA(\mathcal{F})$ denotes the infinitesimal area of the surface $\mathcal{F}$ and H and K are its mean and Gaussian curvature respectively. See also Chapter **??** of this volume.

For quadrilateral surfaces, parallel offset surfaces or equivalently a generalized discrete Gauss map can be used in an analogous way to define Gaussian and mean curvature.

First we note that the oriented area functional $A(P)$ of a planar polygon P is a quadratic form. The corresponding symmetric bilinear form $A(P, Q)$ is called *mixed area*. It will be important for the following theory and may be obtained as follow.

Consider two planar polygons $P = (\mathbf{p}_0, \ldots, \mathbf{p}_{k-1})$ and $Q = (\mathbf{q}_0, \ldots, \mathbf{q}_{k-1})$ with vertices $\mathbf{p}_i$ and $\mathbf{q}_i$ respectively and whose corresponding edges are parallel. Then $A(P, Q) = \frac{1}{2}(A(P+Q) - A(P) - A(Q))$ where $P+Q = (\mathbf{p}_0+\mathbf{q}_0, \ldots, \mathbf{p}_{k-1}+\mathbf{q}_{k-1})$ is the polygon obtained by pointwise addition. For further use, we express the mixed area using the determinant. Let $\mathbf{n}$ be the unit normal vector of the parallel planes containing the polygons P and Q. Then

$$A(P, Q) = \frac{1}{4}\sum_{j=0}^{k-1}[\det(\mathbf{p}_j, \mathbf{q}_{j+1}, \mathbf{n}) + \det(\mathbf{q}_j, \mathbf{p}_{j+1}, \mathbf{n})]. \tag{2}$$

Given a line congruence net (F, N), consider one quadrilateral face f with area $A(f) \neq 0$. Denote by n the corresponding face of the surface N. Then the

one parameter family of parallel offset faces is $f_t = f + tn$ for $t \in \mathbb{R}$. The area of f_t is

$$A(f_t) = A(f + tN, f + tN) = \left(1 + 2t\frac{A(f,n)}{A(f)} + t^2\frac{A(n)}{A(f)}\right) A(f). \tag{3}$$

Comparing this equation with the corresponding formula for smooth surfaces (1) leads to the following curvature definitions on faces, see [25, 4].

Definition 2.5. Let (F, N) be a line congruence net such that the faces of F are not degenerate, i.e. $A(f) \neq 0$. Then the *discrete Gaussian curvature* K and the *discrete mean curvature* H are defined by

$$K = \frac{A(n)}{A(f)} \qquad \text{and} \qquad H = -\frac{A(f,n)}{A(f)}. \tag{4}$$

Here f denotes a quadrilateral face of F and n is the corresponding face of N.

Note that the Gaussian curvature is defined as the quotient of the areas of the Gauss image and of the original surface analogously as in the smooth case. Moreover, as for a quadrilateral surface with a line congruence the generalized Gauss map is only defined up to a common factor, the curvatures at faces are also defined up to multiplication by a common constant.

The principle curvatures κ_1, κ_2 are in the smooth case defined by the formulas $H = (\kappa_1 + \kappa_2)/2$ and $K = \kappa_1\kappa_2$ as the zeros of the quadratic polynomial $(1 - 2tH + t^2K) = (1 - t\kappa_1)(1 - t\kappa_2)$.

Discrete principle curvatures can be defined in an analogons way in the following case. Let (F, N) be a line congruence net such that all faces of F are non-degenerate and all quadrilaterals of F are convex (or equivalently all quadrilaterals of N are convex), that is the vertices of every face are on the boundary of their convex hull. Then the *discrete principle curvatures* κ_1, κ_2 on the faces are the zeros of the quadratic polynomial $(1 - 2tH + t^2K) = (1-t\kappa_1)(1-t\kappa_2)$ where H and K are the discrete mean and the discrete Gaussian curvature respectively. Note that in this case $H^2 - K \geq 0$ and Minkowski's first inequality $A(f,n)^2 - A(f)A(n) \geq 0$ applies, see [29].

Using these definitions, one easily obtains special classes of quadrilateral surfaces. This article focuses on discrete minimal surfaces:

Definition 2.6. A line congruence net (F, N) is called a *discrete minimal surface* if $H = 0$ for all faces.

2.2 Characterization of discrete minimal surfaces

Lemma 2.7. *A line congruence net (F, N) is a discrete minimal surface if and only if the mixed areas vanish, $A(f, n) = 0$, for all quadrilaterals f of F and the corresponding quadrilaterals n of N.*

Thus, we first study planar quadrilaterals P, Q with parallel edges whose mixed area vanishes, $A(P, Q) = 0$, and which are called *dual*.

Lemma 2.8. *For every planar quadrilateral there exists a dual one. For non-zero quadrilaterals the dual is unique up to scaling and translation.*

Furthermore two planar quadrilaterals $P = (\mathbf{p}_0, \ldots, \mathbf{p}_3)$ and $Q = (\mathbf{q}_0, \ldots, \mathbf{q}_3)$ with parallel corresponding edges are dual to each other if and only if their diagonals are antiparallel, that is $\mathbf{p}_2 - \mathbf{p}_0 \parallel \mathbf{q}_3 - \mathbf{q}_1$ and $\mathbf{p}_3 - \mathbf{p}_1 \parallel \mathbf{q}_2 - \mathbf{q}_0$.

Proof. In the following, we will only consider quadrilaterals with non-zero edges. The degenerate cases can easily be treated using projective geometry.

We first show the characterization of dual quadrilaterals by their diagonals. Using equation (2) and and the multilinearity of the determinant we obtain

$$4A(P,Q) = \det(\mathbf{p}_0 - \mathbf{p}_2, \mathbf{q}_1 - \mathbf{q}_3, \mathbf{n}) + \det(\mathbf{p}_1 - \mathbf{p}_3, \mathbf{q}_2 - \mathbf{q}_0, \mathbf{n}).$$

As corresponding edges $\mathbf{p}_{i+1} - \mathbf{p}_i$ and $\mathbf{q}_{i+1} - \mathbf{q}_i$ (for indices (mod 4)) are parallel, we further deduce

$$\det(\mathbf{p}_0 - \mathbf{p}_2, \mathbf{q}_1 - \mathbf{q}_3, \mathbf{n}) = \det(\mathbf{p}_1 - \mathbf{p}_3, \mathbf{q}_2 - \mathbf{q}_0, \mathbf{n}),$$

which proves the claim.

The conditions of antiparallel diagonals for dual quadrilaterals show the uniqueness claim, as Q is already fixed by specifying $\mathbf{q}_0 \in \mathbb{R}^3$ and a common scaling factor $\lambda \neq 0$.

Existence of a quadrilateral dual to a non-zero quadrilateral P can be seen as follows. Let $\mathbf{m}$ be the intersection point of the diagonals of P and define the two diagonal directions

$$e_1 = \frac{\mathbf{p}_0 - \mathbf{m}}{\|\mathbf{p}_0 - \mathbf{m}\|} = -\frac{\mathbf{p}_2 - \mathbf{m}}{\|\mathbf{p}_2 - \mathbf{m}\|} \quad \text{and} \quad e_2 = \frac{\mathbf{p}_1 - \mathbf{m}}{\|\mathbf{p}_1 - \mathbf{m}\|} = -\frac{\mathbf{p}_3 - \mathbf{m}}{\|\mathbf{p}_3 - \mathbf{m}\|}.$$

Set

$$Q^* = (\mathbf{q}_0^*, \dots, \mathbf{q}_3^*) := \left(-\frac{e_2}{\|\mathbf{p}_0 - \mathbf{m}\|}, -\frac{e_1}{\|\mathbf{p}_1 - \mathbf{m}\|}, \frac{e_2}{\|\mathbf{p}_2 - \mathbf{m}\|}, \frac{e_1}{\|\mathbf{p}_3 - \mathbf{m}\|} \right).$$

Then Q^* is a planar quadrilateral whose diagonals are antiparallel to those of P by construction. Furthermore, the edges of Q^* are parallel to the corresponding edges of P. We just show this for one edge as the other cases are analogous.

$$\mathbf{q}_1^* - \mathbf{q}_0^* = -\frac{e_1}{\|\mathbf{p}_1 - \mathbf{m}\|} + \frac{e_2}{\|\mathbf{p}_0 - \mathbf{m}\|} = \frac{\mathbf{p}_1 - \mathbf{p}_0}{\|\mathbf{p}_0 - \mathbf{m}\|\|\mathbf{p}_1 - \mathbf{m}\|}$$

□

Although dual quadrilaterals always exist locally, global dualization requires additional properties in order to result again in a surface.

Definition 2.9. A quadrilateral surface $F : \mathscr{D} \to \mathbb{R}^3$ is called a *discrete Koenigs net* if it admits a dual net $F^* : \mathscr{D} \to \mathbb{R}^3$, i.e. F^* is a quadrilateral surface such that corresponding quadrilaterals of F and F^* are dual.

There are further characterizations of Koenigs nets, in particular in projective geometry, see for example [7, Chapter 2.3] for more details.

Theorem 2.10. *Let F be a discrete Koenigs net. Then the line congruence net (F, N) with $N = F^*$ is a discrete minimal surface.*

Proof. By Lemma 2.7 we know that $H = 0$ is equivalent to $A(f, n) = 0$ for all corresponding faces f of F and n of N. This holds by the definition of the dual surface $N = F^*$. □

For smooth minimal surfaces $\mathcal{F}$ the characterization $\mathcal{N} = \mathcal{F}^*$ for the Gauss map $\mathcal{N}$ is due to Christoffel [12], for a modern treatment see for example [18].

In order to obtain a discrete Gauss map N which is related to the unit sphere $\mathbb{S}^2$ as for its smooth analogon, one may consider spherical polyhedra. There are three natural types of such polyhedra with

- vertices on $\mathbb{S}^2$:

  In this case $\|N(v)\| = 1$ and for all parallel surfaces $F_t = F + tN$ the distance between corresponding vertices is constant.
  Furthermore, we obtain a *circular net* $N : \mathcal{D} \to \mathbb{S}^2$, that is for every quadrilateral exists a circle through its vertices. The dual net $F = N^*$ is then also a circular net, see [7] for a proof and more details.

- faces tangent to $\mathbb{S}^2$:

  In particular, for every vertex of the polyhedron the incident faces are tangent to a cone of revolution touching $\mathbb{S}^2$. Thus we have a *conical net* and this property is conserved by dualization, see [25] for more details.

- edges tangent to $\mathbb{S}^2$, called *Koebe polyhedra*:

  In this case every face of N intersects $\mathbb{S}^2$ in a circle which touches the boundary edges of the face from inside.

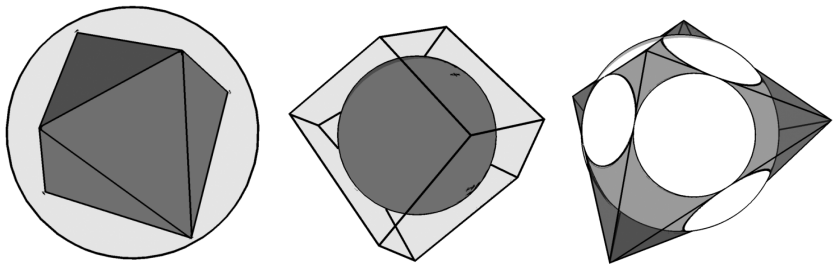

Figure 4: Three possible types of spherical polyhedra

Note that from circular nets in $\mathbb{S}^2$ one obtains discrete minimal surfaces which have been defined in [2]. Moreover, circular nets belong to Moebius geometry whereas conical nets are part of Laguerre geometry.

In the following, we will only consider Koebe polyhedra further. These are closely connected to the theory of circle patterns. Above, we have already identified a family of touching circles on $\mathbb{S}^2$ corresponding to the faces of the Koebe polyhedron. There is another family of circle corresponding to the vertices. Consider every vertex of the Koebe polyhedron as the apex of a cone which touches $\mathbb{S}^2$. The intersections of the cones with $\mathbb{S}^2$ are circles which touch at points where the edges of the Koebe polyhedron touch $\mathbb{S}^2$. Moreover, the circles corresponding to faces intersect the circles corresponding to vertices orthogonally at these touching points.

Conversely, to an orthogonal circle pattern in $\mathbb{S}^2$ we can associated a Koebe polyhedron by choosing one family of touching circles as above and adding the corresponding cones. Their apices are the vertices of the polyhedron which are

by construction connected by edges touching $\mathbb{S}^2$. Thus to an orthogonal circle pattern there are associated two corresponding Koebe polyhedra.

Furthermore, instead of cones, we may consider the spheres with centers at the vertices of a Koebe polyhedron which intersect $\mathbb{S}^2$ orthogonally. This also leads to the same family of circles as for the touching cones. Also, Koebe polyhedra are thus discrete S-isothermic surface which were originally introduced in [3] and will be explained in the following.

Definition 2.11. Let $\mathscr{D}$ be a bipartite quad-graph, that is the vertices are colored white and black such that every edge is incident to one white and one black vertex. $\mathscr{D}$ is called a *S-quad-graph* if all interior black vertices have degree 4 and if the white vertices can be labelled Ⓒ and Ⓢ in such a way that each quadrilateral has one white vertex labelled Ⓒ and one white vertex labelled Ⓢ. Furthermore, the Ⓒ-labelled white vertices have degree 4 and the Ⓢ-labelled white vertices have even degree.

Let $\mathscr{D}$ be an S-quad-graph and let $V_b(\mathscr{D})$ be the set of all black vertices. A *discrete S-isothermic surface* is a map $F_b : V_b(\mathscr{D}) \to \mathbb{R}^3$ with the following properties:

(i) If $v_1, \dots, v_4 \in V_b(\mathscr{D})$ are the neighbors of a Ⓒ-labelled vertex in cyclic order, then $F_b(v_1), \dots, F_b(v_4)$ lie on a circle in $\mathbb{R}^3$ in the same cyclic order. This defines a map from the Ⓒ-labelled white vertices to the set of circles in $\mathbb{R}^3$.

(ii) If $v_1, \dots, v_{2m} \in V_b(\mathscr{D})$ are the neighbors of a Ⓢ-labelled vertex in cyclic order, then $F_b(v_1), \dots, F_b(v_{2m})$ lie on a sphere in $\mathbb{R}^3$. This defines a map from the Ⓢ-labelled white vertices to the set of spheres in $\mathbb{R}^3$.

(iii) If v_c and v_s are the Ⓒ-labelled and the Ⓢ-labelled vertices of a quadrilateral of $\mathscr{D}$, the circle corresponding to v_c intersects the sphere corresponding to v_s orthogonally.

Given an S-quad-graph $\mathscr{D}$, we can construct an associated graph $\mathscr{D}_{Ⓢ}$ by taking as vertices all Ⓢ-labelled white vertices. Two such vertices are connected by an edge in $\mathscr{D}_{Ⓢ}$ if they are incident to the same black vertex in $\mathscr{D}$. If $F_b : V_b(\mathscr{D}) \to \mathbb{R}^3$ is a discrete S-isothermic surface, the *central extension* of F_b is the discrete quadrilateral surface $F : V(\mathscr{D}_{Ⓢ}) \to \mathbb{R}^3$ defined by

$$F(v) = \text{the center of the sphere corresponding to } v.$$

By abuse of notation, we also call F a discrete S-isothermic surface.

Theorem 2.12. *Every discrete S-isothermic surface is a Koenigs net (i.e. dualizable).*

Proof. As the vertices of the quad-graph $\mathscr{D}_{Ⓢ}$ have even degree, the edges can be labelled $+$ and $-$ such that opposite edges of every quadrilateral carry the same label. Given the centers of spheres c and the radii r of a discrete S-isothermic surface F, define new centers of spheres c^* and radii r^* by

$$r^*(v) = \frac{1}{r(v)} \qquad \text{and} \qquad c^*(v_1) - c^*(v_0) = \pm \frac{c(v_1) - c(v_0)}{r(v_1) r(v_0)}, \tag{5}$$

where the sign $\pm$ is given by the label of the edge $[v_1, v_0] \in E(\mathscr{D}_{\textcircled{S}})$.

We first show that this definition leads indeed to a quadrilateral surface F^*. In particular, we need to show that for any quadrilateral of F we get a new corresponding quadrilateral of F^* by (5). Let c_0, c_1, c_2, c_3 and r_0, r_1, r_2, r_3 be the centers of spheres and the corresponding radii of a quadrilateral of F enumerated in counterclockwise orientation. By assumption there is a circle inscribed in this quadrilateral with center m and radius R. It touches the boundary edges at the points $p_{01}, p_{12}, p_{23}, p_{30}$ where $p_{ij} = c_i + r_i \frac{c_j - c_i}{r_i + r_j}$ are images of black vertices. See Figure 5. Note that the quadrilaterals $P_i = (c_i, p_{i,i+1}, m, p_{i-1,i})$, where all indices are taken $\pmod 4$, are orthogonal rhombi. Now scale P_i by

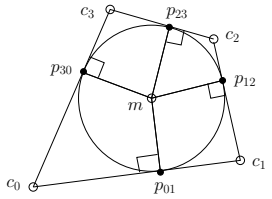

Figure 5: A quadrilateral face of an S-isometric surface

$1/(Rr_i)$ and reflect it in the edge labelled $+$. The new orthogonal rhombi P_i^* then have two edges of length $1/R$ and another two of length $r_i^* = 1/r_i$. By suitable translations these orthogonal rhombi P_i^* may be combined into a new quadrilateral face with an inscribed circle with radius $1/R$. The corresponding vertices $c_0^*, \dots, c_3^*$ of this quadrilateral then satisfy (5) by construction and $\|c_{i+1}^* - c_i^*\| = r_{i+1}^* + r_i^*$ for the radii $r_0^*, \dots, r_3^*$.

Therefore it remains to show that corresponding quadrilaterals of F and F^* are dual. Using the above notations, it is by Lemma 2.8 sufficient to show that

$$c_1^* - c_3^* \parallel c_2 - c_0 \iff c_1^* - c_0^* + c_0^* - c_3^* \parallel c_2 - c_0,$$

where $\parallel$ means that the vectors are parallel. By the definition of c^* this condition is equivalent to

$$\frac{c_1 - c_0}{r_0 r_1} + \frac{c_3 - c_0}{r_3 r_0} \parallel c_2 - c_0. \tag{6}$$

As F^* is a quadrilateral surface, we have with the definition of c^*

$$\begin{aligned} &\frac{1}{r_0}\left(\frac{c_1 - c_0}{r_1} + \frac{c_3 - c_0}{r_3}\right) = \frac{1}{r_2}\left(\frac{c_2 - c_3}{r_1} + \frac{c_2 - c_1}{r_3}\right) \\ \iff &\left(\frac{1}{r_1} + \frac{1}{r_3}\right)(c_2 - c_0) = \left(\frac{r_2}{r_0} + 1\right)\left(\frac{c_1 - c_0}{r_1} + \frac{c_3 - c_0}{r_3}\right). \end{aligned}$$

This immediately shows that condition (6) holds. □

Definition 2.13. An *S-isothermic discrete minimal surface* (or discrete minimal surface of Koebe type) is an S-isothermic discrete surface $F : V(\mathscr{D}_{\textcircled{S}}) \to \mathbb{R}^3$ whose dual surface is a Koebe polyhedron.

The *associated family* F_φ of an S-isothermic discrete minimal surface F_0 consists of the one-parameter family of discrete surfaces that are obtained by the following construction. Before dualizing the Koebe polyhedron, rotate each edge by an equal angle φ in the plane which is tangent to the unit sphere in the point where the edge touches the unit sphere, see Figure 6.

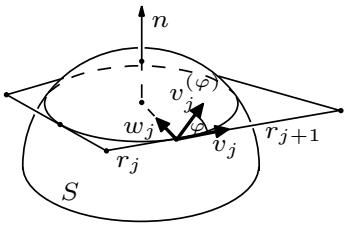

Figure 6: The vector $v_j^{(\varphi)}$ is obtained by rotating v_j in the tangent plane to the sphere S at c_j.

This definition implies that the discrete associated family keeps essential properties of the smooth associated family. In particular, the surfaces are isometric and have the same Gauss map.

Theorem 2.14 ([1, Theorem 8])**.** *The discrete surfaces F_φ of the associated family of an S-isothermic discrete minimal surface F_0 consist of touching spheres. The radii of the spheres do not depend on φ.*

In the generic case, when the S-quad-graph is a part of the regular square grid, there are also circles through the points of contact. The normals of these circles do not depend on φ.

3 Construction of Koebe polyhedra and discrete minimal surfaces

Definition 2.13 leads to the following *construction scheme* for discrete minimal analogs of known smooth minimal surfaces, see also [1].

Step 1: Consider a smooth minimal surface together with its conformal curvature line parameterization. Map the curvature lines to the unit sphere by the Gauss map to obtain a qualitative picture. The goal is to *understand the combinatorics of the curvature lines.*

From the combinatorial picture of the curvature lines we choose finitely many curvature lines to obtain a finite cell decomposition of the unit sphere $\mathbb{S}^2$ (or of a part or of a branched covering of $\mathbb{S}^2$) with quadrilateral cells. The choice of the number of curvature lines corresponds to the level of refinement (and possibly to the choice of different length parameters). Generically, all vertices have degree 4. Exceptional vertices correspond to umbilic or singular points, ends or boundary points of the minimal surface. So the cell decomposition (or a suitable subdivision) leads to an S-quad-graph which provides a *combinatorial conformal parameterization.*

Step 2: Given the combinatorics from step 1, *construct an orthogonal spherical circle pattern* where circles correspond to white vertices of the S-quad-graph. If two vertices are incident to the same face the corresponding two circles intersect orthogonally. Circles corresponding to vertices which are not incident to the same face, but to the same black vertex touch. The interiors of the disks filling such touching circles are

disjoint. At boundary vertices we use information about the smooth minimal surface to specify angles. Ends have also to be taken care of but we do not consider this case further.

Step 3: From the circle pattern, *construct the Koebe polyhedron.* Choose half of the circles, that is those corresponding to white vertices labelled ⓒ or those labelled ⓢ. The two choices lead to different discrete surfaces close to each other. Take these circles and build the spheres which intersect $\mathbb{S}^2$ orthogonally in these circles. Then build the Koebe polyhedron by joining the apices corresponding to touching circles.

Step 4: *Dualize the Koebe polyhedron* to arrive at the desired discrete minimal surface.

Note that we obtain the geometry (discrete minimal surface) from the combinatorics of the curvature lines (and eventually some boundary conditions). Therefore the first two steps are most important and may require some care. In Section 3.2, we present some more details on how to find the combinatorics of the curvature lines and the boundary conditions for the concrete examples presented in Section 4. Also note that the dualization may be impossible for the whole Koebe polyhedron. Then we first cut the polyhedron along suitable edges.

3.1 Construction of Koebe polyhedra and spherical circle patterns

Given the combinatorics, there remains the task to construct the corresponding spherical circle pattern and the Koebe polyhedron. The existence of Koebe polyhedra was first studied by Koebe [20]. There are several generalizations of Koebe's theorem, for example

Theorem 3.1. *Every polytopal cell decomposition of the sphere can be realized by a polyhedron with edges tangent to the sphere. This realization is unique up to projective transformations which fix the sphere.*

A proof of this theorem has been given in [9], see also [31, 28, 5] for generalizations. [5] contains a variational proof. A suitable stereographic projection of the orthogonal circle pattern on $\mathbb{S}^2$ which corresponds to the sought-after polyhedron is shown to be the critical point of a strictly convex functional. This implies existence and uniqueness. By its explicit formula the functional is also easy to compute and therefore particularly suitable for explicit constructions. Furthermore, an adaption of the functional can be used to compute planar circle patterns with given angles at boundary vertices corresponding to Neumann boundary conditions.

As orthogonal circle patterns are crucial for our construction, we specify this notion.

Definition 3.2. Let $\mathscr{D}$ be a bipartite quad-graph. Let G be the associated graph constructed from all white vertices of $\mathscr{D}$, that is $V(G) = V_w(\mathscr{D})$. Two vertices of G are connected by an edge if they are incident to the same face in $\mathscr{D}$.

An *orthogonal planar circle pattern for $\mathscr{D}$ or G* is a configuration of circles in the complex plane $\mathbb{C}$, such that to each white vertex of $V_w(\mathscr{D}) = V(G)$ there corresponds a circle (all with the same orientation). If two white vertices are incident to the same face in $\mathscr{D}$, i.e. are incident in G, the corresponding circles intersect orthogonally. Furthermore, if two white vertices are incident to the same black vertex of $V_b(\mathscr{D})$, but are not incident to the same face in $\mathscr{D}$, the corresponding circles touch and have disjoint interiors.

Remark 3.3. Note that an orthogonal planar circle pattern for $\mathscr{D}$ exists only if all black vertices have degree 4. For the graph G this means that all faces are quadrilaterals.

The notion of orthogonal circle patterns may easily be generalized, for example to spherical or hyperbolic geometry. Accordingly, a *spherical orthogonal circle pattern for $\mathscr{D}$ or G* is a configuration of circles on the sphere S^2 intersecting orthogonally corresponding to the combinatorics of $\mathscr{D}$ or G respectively analogously as for an orthogonal planar circle pattern. In other terms, spherical orthogonal circle patterns for $\mathscr{D}$ or G and orthogonal planar circle patterns for $\mathscr{D}$ or G are related by a suitable orthogonal projections.

Theorem 3.4. *Let $\mathscr{D}$ be a strongly regular cell decomposition of a compact oriented surface with or without boundary which is a bipartite quad-graph. Let G be the associated graph built from all white vertices. Let $\Phi \in (0,\infty)^V$ be a function on the set $V = V(G)$ of vertices of G which correspond to the white vertices of $\mathscr{D}$ such that $\Phi(v) = 2\pi$ for interior vertices $v \in V(G)$. Φ prescribes for boundary vertices of G the Neumann boundary conditions. A planar orthogonal circle pattern corresponding to these data exists if and only if the following condition is satisfied:*

If $V' \subseteq V$ is any nonempty set of vertices and $E' \subseteq E = E(G)$ is the set of all edges which are incident with any vertex $v \in V'$, then

$$\sum_{v \in V'} \Phi(v) \leq \sum_{e \in E'} \pi,$$

where equality holds if and only if $V' = V$.

If it exists, the orthogonal circle pattern is unique up to similarities.

See [5] for a proof of a more general statement.

Theorem 3.4 is useful for the application of Step 2 of our construction scheme above as we usually do not obtain in Step 1 a cell decomposition of the whole sphere but only of a part. In order to construct the Koebe polyhedron, the main task is to suitably specify the corresponding boundary conditions after stereographic projection.

However, for the examples presented in Section 4 the boundary conditions are simplest for the *spherical* circle patterns. Therefore, we have actually used a method developed by Springborn for calculating the spherical circle patterns directly by a variational principle, see [1, Section 8] or [34] for more details. The solutions of the spherical circle pattern problem with given boundary angles are in one-to-one correspondence with the critical points of another functional. Since this functional is not convex and has negative index at least one, the critical points cannot be obtained by simply minimizing the functional. In order to numerically compute the spherical circle pattern, a convenient reduced

functional is used instead. Existence and uniqueness of a solution are not yet proven. Nevertheless, this method has proven to be amazingly powerful, in particular to produce the spherical circle patterns for the examples in Section 4. More details concerning the implementation can be found in [33].

3.2 Construction of S-isothermic discrete minimal surfaces with special boundary conditions

In the following we explain some details of how to perform the first step (finding the combinatorial parametrization and boundary conditions) of the general constructions scheme for S-isothermic discrete minimal surfaces. We restrict ourselves to examples with boundary conditions specified below (Schwarzian chains).

3.2.1 Boundary conditions and reduction of symmetries

We consider the family of smooth minimal surfaces which are bounded by a closed curve consisting of finitely many arcs of positive length each of which

either (i) *lies within a plane which intersects the surface orthogonally.* Then this boundary arc is a curvature line and the surface may be continued smoothly across the plane by reflection in this plane.

or (ii) *lies on a straight line.* Then this boundary arc is an asymptotic line and the surface may be continued smoothly across this straight line by 180°-rotation about it.

In each case the image of the boundary arc under the Gauss map is (a part of) a great circle on the unit sphere. The implications in (i) and (ii) are well-known properties of smooth minimal surfaces (Schwarz's reflection principles); see for example [14].

Since the boundary conditions are translated into angle conditions for boundary circles, an S-isothermic discrete minimal surface may also be continued by reflection in the boundary planes or by 180°-rotation about straight boundary lines. In particular, the boundary circles of the spherical circle pattern intersect the corresponding great circle orthogonally.

Thus in order to simplify the construction of a discrete analog, we only consider a *fundamental piece* of the smooth (and the discrete) minimal surface. This piece of the surface is bounded by planar curvature lines and/or straight asymptotic lines (like the whole surface itself) and the whole surface is obtained from the fundamental piece by successive reflection/rotation in its boundary planes/lines and the new obtained boundary planes/lines. Furthermore, there is no strictly smaller piece with this property.

3.2.2 Combinatorics of curvature lines

Given a fundamental piece of a smooth minimal surface, first determine

- a combinatorial picture of the image of the boundary arcs under the Gauss map (which are parts of great circles on $\mathbb{S}^2$),
- the angles between different boundary arcs on $\mathbb{S}^2$,

- and eventually the lengths of the boundary arcs on $\mathbb{S}^2$ if the angles do not uniquely determine the boundary curve on $\mathbb{S}^2$ (up to rotations of the sphere). This case is more difficult; see Remark 3.5.

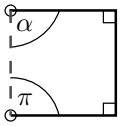

——	curvature line	angles of the boundary
– –	asymptotic line	configuration on $\mathbb{S}^2$:
○	umbilic point	⌝ = right angle, $\alpha = \pi/3$

Figure 7: A combinatorial picture of the boundary conditions on $\mathbb{S}^2$ of a fundamental piece of Schwarz's H surface.

Second, from the smooth curvature line parametrization we deduce the following conditions.

(1) Umbilic and singular points are taken from the smooth minimal surface, but only their combinatorial locations matter. The smooth surface also determines the number of curvature lines meeting at these points. For interior umbilic or singular points, we additionally have to take care how many times the interior region is covered by the Gauss map. This case does not occur in any of the examples presented in Section 4, so we assume for simplicity that all umbilic or singular points lie on the boundary.

(2) At a regular intersection point of a boundary curvature line and a boundary asymptotic line possibly additional curvature lines are taken from the smooth surface (depending on the intersection angle).

(3) The curvature lines of the combinatorial parametrization divide the domain into combinatorial squares. The only exceptions are combinatorial triangles formed by two curvature lines and by an asymptotic line on the boundary.

Hence, first determine all special points from conditions (1) and (2) and continue the additional curvature line(s) meeting at these points. In this way, the combinatorial domain is divided into finitely many subdomains such that condition (3) holds and the discrete curvature lines correspond to or approximate the smooth (infinite) curvature line pattern; see Figure 8 (left).

Given this coarse subdivision the parametrization of the subdomains is obvious. The only additional conditions occur at common boundaries of two subdomains, where the number of crossing curvature lines has to be equal on both sides. The remaining free integer parameters of the discrete minimal surface correspond to smooth parameters of the continuous minimal surface such as scaling or quotients of lengths (for example of the boundary curves).

Remark 3.5. By construction, the free parameters of the combinatorial curvature line parametrization take integer values and the number of (quadrilateral) subdomains is finite. Also, all combinatorial curvature lines are closed modulo the boundary. In general these properties do not hold for curvature lines of smooth minimal surfaces. Furthermore, there may be dependencies between the numbers of curvature lines of different types which have to be approximated by the choice of the free integer parameters of the combinatorial curvature line

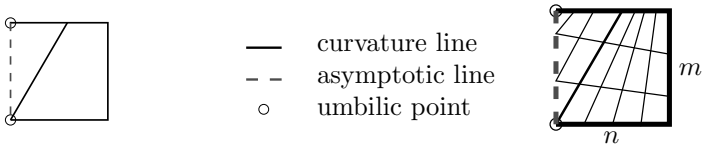

Figure 8: A combinatorial conformal parametrization of a fundamental domain of Schwarz's H surface.

parametrization. These three aspects affect the different appearances of the smooth minimal surfaces and its discrete minimal analog.

In the special case that the smooth curvature lines are closed modulo the boundary and the combinatorial curvature line parametrization has only one free parameter (corresponding to overall scaling), the discrete minimal analog will have exactly the same boundary planes/straight lines (up to translation and scaling). In this way we can construct some triply-periodic S-isothermic discrete minimal analogs to triply-periodic minimal surfaces.

4 Examples of discrete minimal surfaces

In the following, the construction of discrete minimal surfaces explained in Sections 3 and 3.2 is applied to some examples. In each case we present the boundary conditions and deduce suitable reduced conditions, a combinatorial picture of the curvature and/or the asymptotic lines and the image of the reduced boundary conditions under the Gauss map. If this image is uniquely determined by the intersection angles between arcs of great circles (up to rotation of the sphere), then the corresponding spherical circle pattern will also be unique (due to the simple combinatorics). This is the case in 4.1–4.6, for symmetric quadrilaterals and for the cubic frames considered in 4.7.3. Reflection in straight boundary lines and/or boundary planes results in triply periodic discrete minimal surfaces analogously as for smooth surfaces. This is the case in 4.3–4.6 without generalizations and in 4.1, 4.2 and 4.7.3 for special cases. The Figures often show one cubical unit cell of the periodic lattice.

Pictures of the corresponding smooth minimal surfaces can be found in textbooks like [14, 23], in [19], on Brakke's web-page [8], or in some of the original treatises cited below.

Notation. For the combinatorial pictures of the curvatures lines we use the following notation.

——	curvature line	Angles of the boundary configuration on $\mathbb{S}^2$:	
– –	asymptotic line		
○	umbilic point	⌝	right angle
n,m,k,l	integer parameters of curvature or asymptotic lines	$\alpha, \beta, \gamma, \delta, \eta$	given angles

4.1 Gergonne's surface

Gergonne's surface traces back to J. D. Gergonne [17], who posed the first geometric problem leading to minimal surfaces with free boundaries in 1816. A correct solution was only found by H. A. Schwarz in 1872; see [32, pp. 126–148].

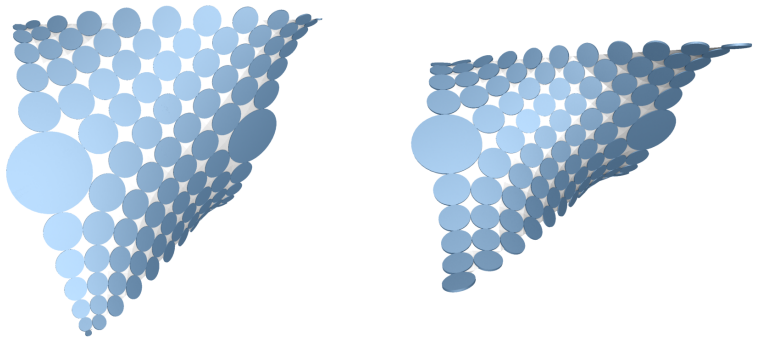

Figure 9: Discrete Gergonne's surface with $\alpha = \frac{\pi}{6}$ (left, case 3 of Figure 10(d) with $m = 1, n = 3$) and $\alpha = \frac{\pi}{4}$ (right, case 2 of Figure 10(d) with $n = 4$).

Boundary conditions: Given a cuboid take two opposite faces as boundary faces and non-collinear diagonals of two other opposite faces, as in Figure 10(a). Then the two axes of 180°-rotation symmetry (see Figure 10(b)) will lie on the minimal surface and cut it into four congruent fundamental pieces bounded by three straight asymptotic lines and one planar curvature line; see Figure 10(c). Its images under the Gauss map are spherical triangles with angles $\frac{\pi}{2}$, $\frac{\pi}{2}$, and α.

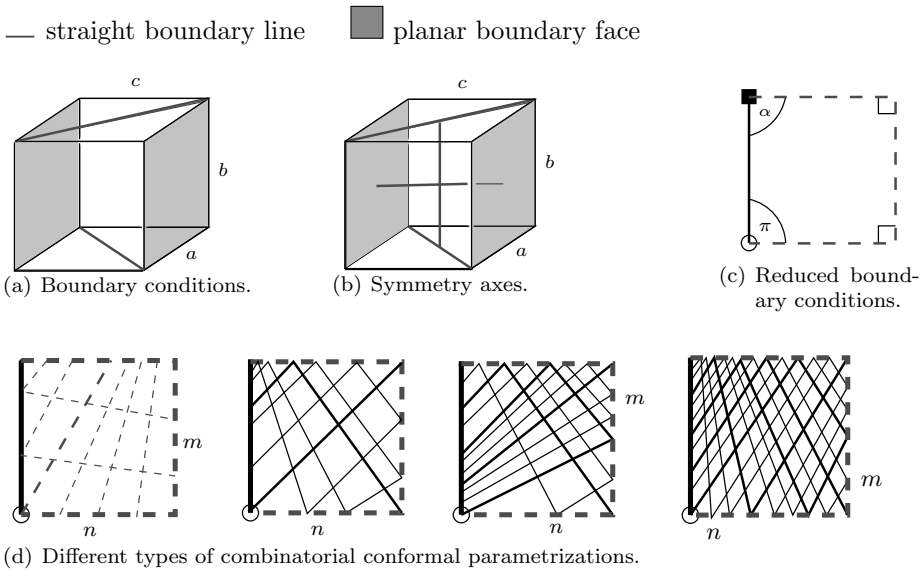

(a) Boundary conditions. (b) Symmetry axes. (c) Reduced boundary conditions.

(d) Different types of combinatorial conformal parametrizations.

Figure 10: Gergonne's surface: boundary conditions and combinatorial conformal parametrizations.

A combinatorial picture of the asymptotic lines or of the curvature lines is shown in Figure 10(d). The two parameters correspond to the free choice of two length parameters of the cuboid, given the angle $(\frac{\pi}{2} - \alpha)$ between the diagonal and the planar boundary face. If $\alpha = \frac{\pi}{4}$, the minimal surface can be continued by reflection and rotation in the boundary faces/edges to result in a triply periodic (discrete) minimal surface.

4.2 Schwarz's CLP surface

Schwarz's CLP surface is one of the triply periodic minimal surfaces already constructed by H. A. Schwarz, see [32, vol. 1, pp. 92–125]. The name CLP is due to A. Schoen [30]. He considered the labyrinth formed by the periodic surface and associated the name to properties of the underlying spatial lattice.

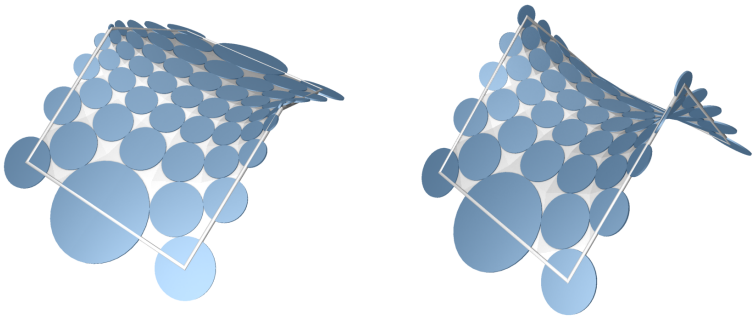

Figure 11: A generalization of Schwarz's CLP surface (left, $\alpha = \frac{2\pi}{3}$, $m = 5, n = 1$) and Schwarz's CLP surface (right, $\alpha = \frac{\pi}{2}$, $m = 5, n = 1$).

Boundary conditions: Consider a frame of two pasted rectangles (with edge lengths a, b, c) which enclose an angle $\alpha \in (0, \pi)$, as in Figure 13 (left). Then there is a plane of reflection symmetry orthogonal to the sides with length a and a corresponding planar curvature line. If $b = c$ there is another plane of reflection symmetry through both corners with angle α and yet another curvature line. This curvature line persists if $b \neq c$. The image of a fundamental domain for the generic case $b \neq c$ under the Gauss map is a spherical triangle with angles $\frac{\pi}{2}$, $\frac{\pi}{2}$, and $(\pi - \alpha)$.

The combinatorics of curvature lines of one fourth of the surface are depicted in Figure 13 (right). The two integer parameters correspond to the two boundary lengths of the first rectangle. Thus for the whole frame there are three parameters corresponding to the three lengths a, b, c. If $\alpha = \frac{\pi}{2}$ the surface can be continued across its boundaries to build a triply periodic discrete minimal surface. Figure 12 shows a cubical unit cell.

4.3 Schwarz's D surface

Schwarz's D surface is another triply periodic minimal surfaces already constructed by H. A. Schwarz, see [32, vol. 1, pp. 92–125]. The surface was named D by A. Schoen because its labyrinth graphs are 4-connected 'diamond' networks.

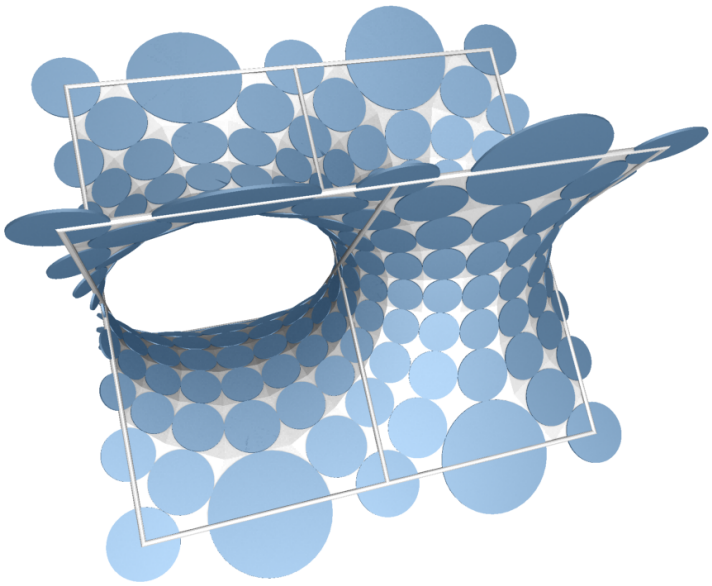

Figure 12: Schwarz's CLP surface

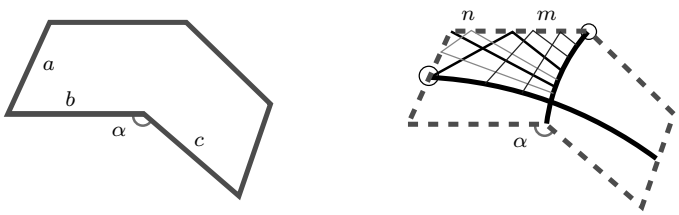

Figure 13: A generalization of Schwarz's CLP surface: boundary frame (left) and combinatorics of curvature lines (right).

Boundary conditions: From the edges of a cuboid take a closed boundary frame as in Figure 15 (left). The three straight lines of 180°-rotation symmetry lying within the minimal surface and one of the three planes of reflection symmetry orthogonal to the boundary frame which give planar curvature lines are depicted in Figure 15 (left). Therefore a fundamental piece is a triangle bounded by two straight asymptotic lines and one planar curvature line. Its image under the Gauss map is a spherical triangle with angles $\frac{\pi}{2}$ (between the two asymptotic lines) and $\frac{\pi}{4}$ and $\frac{\pi}{3}$.

The simple combinatorics of the curvature lines is shown in Figure 15 (right). The only parameter corresponds to overall scaling or refinement.

4.4 Neovius's surface

H. A. Schwarz [32] began to consider minimal surfaces bounded by two straight lines and an orthogonal plane. His student E. R. Neovius continued and deepened this study and found another triply periodic surface, see [22]. This surface

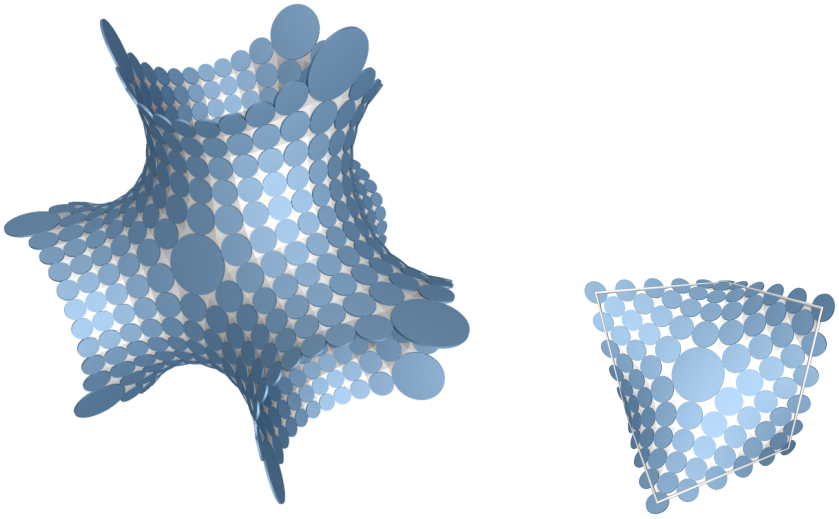

Figure 14: Schwarz's D surface ($n = 4$).

Figure 15: Schwarz's D surface: boundary frame with symmetries (left) and combinatorics of curvature lines of a fundamental piece (right).

has the same symmetry group as Schwarz's P surface and was named C(P) by A. Schoen.

Boundary conditions: One unit cell of the lattice of Neovius's surface is basically a cubical cell with one central chamber and necks out of the middle of each edge of the cube; see Figure 16. By symmetry, it is sufficient to consider one eighth of the unit cell. All the faces of this cuboid are boundary planes and we have the same three planes of reflection symmetry and three lines of 180°-rotation symmetry as for Schwarz's D surface; see Figure 15 (left). Therefore a fundamental piece is a triangle bounded by one straight asymptotic lines and two planar curvature lines. Its image under the Gauss map is a spherical triangle with angles $\frac{3\pi}{4}$ (between the two curvature lines) and $\frac{\pi}{4}$ and $\frac{\pi}{3}$.

The combinatorics of the curvature lines is again very simple, see Figure 17.

4.5 Schwarz's H surface

Schwarz's H surface is another triply periodic minimal surface which was already known to H. A. Schwarz, see [32, vol. 1, pp. 92–125].

Boundary conditions: Take the edges of two parallel copies of an equilateral triangle as boundary frame for a minimal surface spanned in between them, as in Figure 18. Then there are one plane of reflection symmetry parallel to the

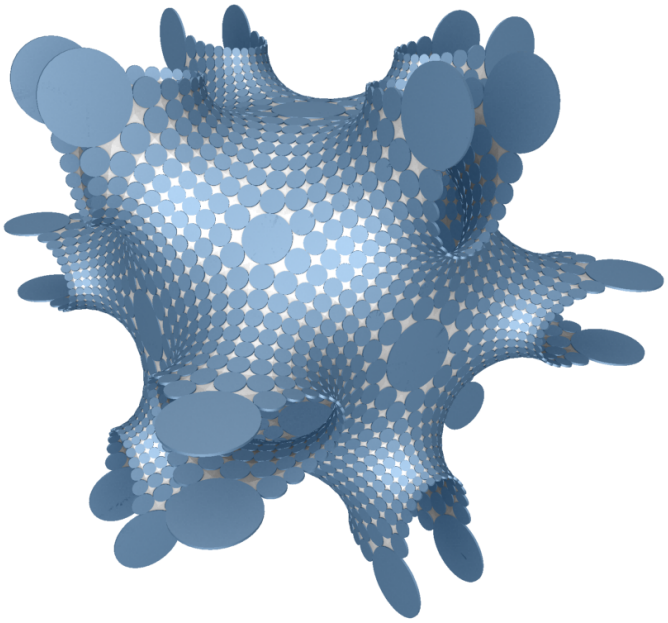

Figure 16: Neovius's surface ($n = 15$).

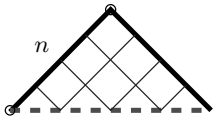

Figure 17: Combinatorics of curvature lines of a fundamental piece of Neovius surface.

triangles and three other orthogonal planes as symmetry group of the equilateral triangle. Thus a fundamental piece is bounded by three planar curvature lines and one straight asymptotic line; see Figure 19(a). Its image under the Gauss map is a spherical triangle with angles $\frac{\pi}{2}$, $\frac{\pi}{2}$, $\frac{\pi}{3}$; see Figure 7.

The combinatorics of the curvature lines is shown in Figure 8 or 19(b). The two parameters correspond to the side length of the equilateral triangle and to their distance.

4.6 Schoen's I-6 surface and generalizations

About 1970, the physicist and crystallographer A. Schoen discovered many triply periodic minimal surfaces. His reports [30] were a bit sketchy, but H. Karcher [19] established the existence of all of Schoen's surfaces.

Boundary conditions: Similarly as for Schwarz's H surface, take the edges of two parallel copies of a rectangle as boundary frame for a minimal surface between them. There are one plane of reflection symmetry parallel to the rectangles and two other orthogonal planes as symmetry group of the rectangle

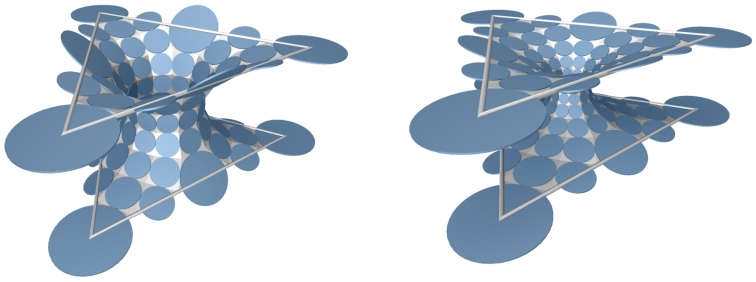

Figure 18: Schwarz's H surfaces with different heights (left: $m = 3, n = 3$, right: $m = 3, n = 6$).

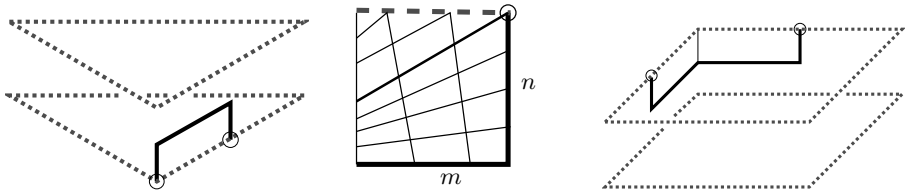

(a) Boundary frame of Schwarz's H surface with a fundamental piece.

(b) Combinatorics of the curvature lines of (one half of) a fundamental piece.

(c) Boundary frame of Schoen's I-6 surface with a fundamental piece.

Figure 19: Schwarz's H surface and (a generalization of) Schoen's I-6 surface.

(four in case of a square). Thus a fundamental piece is generically bounded by three planar curvature lines and one straight asymptotic line; see Figure 19(c). Its image under the Gauss map is a spherical triangle with angles $\frac{\pi}{2}$, $\frac{\pi}{2}$, and $\frac{\pi}{4}$. There is one additional curvature line splitting the piece into two parts which can easily be found be reflection symmetry in the case of squares.

For both parts the combinatorics of curvature lines are the same as for the fundamental piece of Schwarz's H surface; see Figure 19(b) or 8. The three remaining parameters correspond to the side lengths of the two rectangles and to their distance.

In an analogous way to the construction of Schwarz's H surface and Schoen's I-6 surface, we may consider all regular symmetric planar polygons with sides of equal length or to non-regular planar polygons with additional symmetry planes. The fundamental piece is always combinatorially the same as for Schwarz's H surface. The only difference is the angle $\alpha = \frac{\pi}{n}$ for an n-gon. These minimal surfaces may also be understood as an approximation to a piece of the catenoid; see Figure 21 (left). The construction may easily be generalized to further similar examples; see Figure 20 (right) and Figure 21 (right).

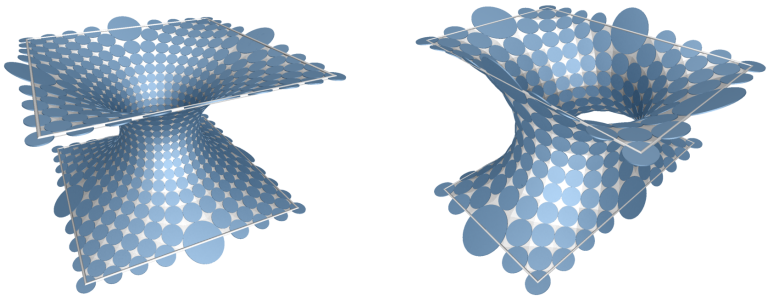

Figure 20: Schoen's I-6 surface (left, $m = 7, n = 14$) and a generalization (right).

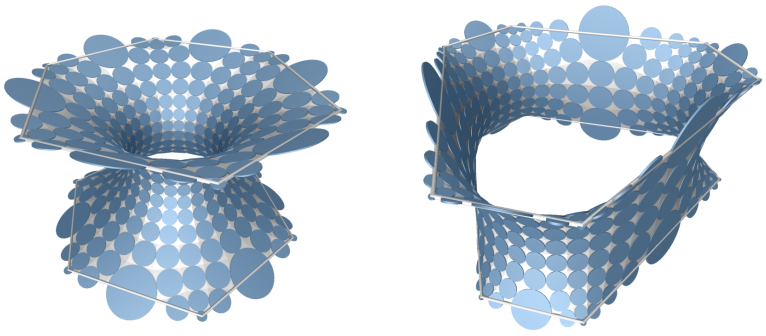

Figure 21: An approximation of a piece of a catenoid using a polygonal boundary frame (left, $n = 10, m = 3$) and a generalization (right, $m_1 = 3, n_1 = 6, m_2 = 7, n_2 = 2$).

4.7 Polygonal boundary frames

As a special class of Plateau's problems, all non-planar, simple, unknotted polygons can be considered as boundary conditions. The main task is to determine the corresponding discrete combinatorics of the conformal parameter lines. The number of different special cases increases with the number of boundary segments, so we confine ourselves to quadrilaterals, pentagons, and a cubical boundary frame as one more complicated example. Since the boundary frame consists only of straight asymptotic lines, we use the conjugate minimal surface from the associated family for the construction, see Definition 2.13.

4.7.1 Quadrilateral

The minimal surface spanned by a quadrilateral with equal side lengths and equal angles of $\frac{\pi}{3}$ was the first known solution in the class of Plateau's problems. In 1865, H. A. Schwarz found the explicit solution [32, pp. 6–125]. About the

same time, B. Riemann independently solved this problem [27, pp. 326–329]. His paper [26] appeared posthumously in 1867. At the same time H. A. Schwarz sent his prize-essay to the Berlin Academy. Later on, Plateau's problem was tackled for other polygonal boundaries, see for example the historical remarks in [14, 23].

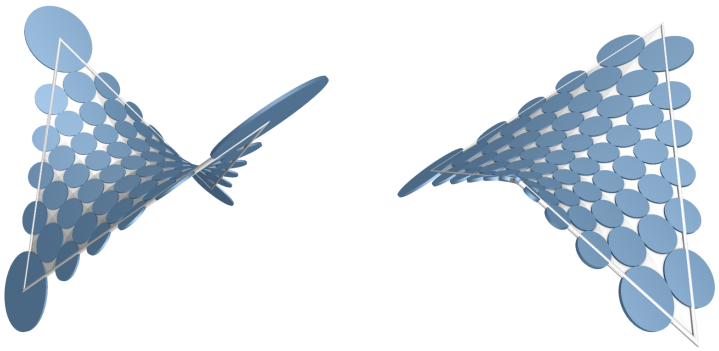

Figure 22: Two examples of discrete quadrilateral boundary frames: a symmetric version (left with $\alpha = \beta = \gamma = \pi/6$, $n = 9$) and a general version (right).

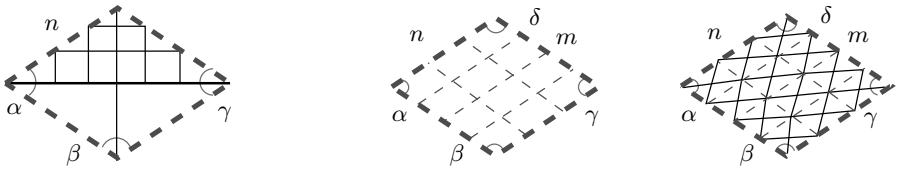

(a) Symmetric quadrilateral. (b) General quadrilateral.

Figure 23: Boundary conditions and combinatorial parametrizations for symmetric and general quadrilaterals.

Given a non-planar quadrilateral of straight boundary lines, the combinatorics of asymptotic lines is easily found; see Figure 23(b) (left). Then the corresponding curvature lines may also be determined, as in Figure 23(b) (right). The two parameters correspond to a global scaling and the to a ratio of lengths of the boundary segments. As explained in Remark 3.5, in general we do not obtain exactly a given quadrilateral boundary frame but an approximation which converges for a suitable choice of parameter values.

In the case of a non-planar symmetric quadrilateral the combinatorics of curvature lines are obvious; see Figure 23(a). The only parameter corresponds to a global scaling or refinement. Thus we can obtain any symmetric quadrilateral boundary frame as the exact boundary of a discrete minimal surface.

4.7.2 Pentagon

In the symmetric case the boundary configuration allows a plane of mirror symmetry containing one boundary vertex and cutting the opposite edge. The re-

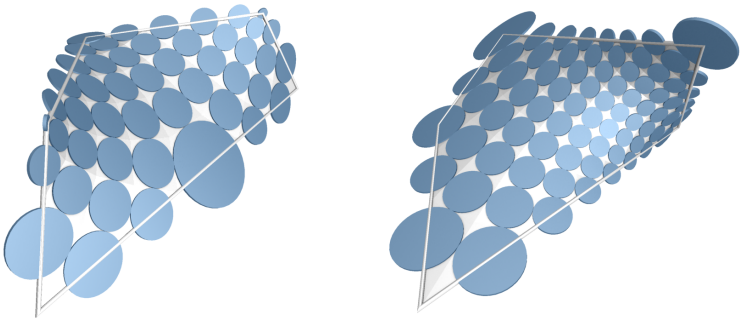

Figure 24: Two examples of discrete pentagons: a symmetric boundary frame (left, $m = 4, n = 4$) and a general boundary frame (right).

maining reduced domain is similar to the boundary conditions of Gergonne's surface and thus has the same combinatorics of asymptotic lines; see Figure 25(a).

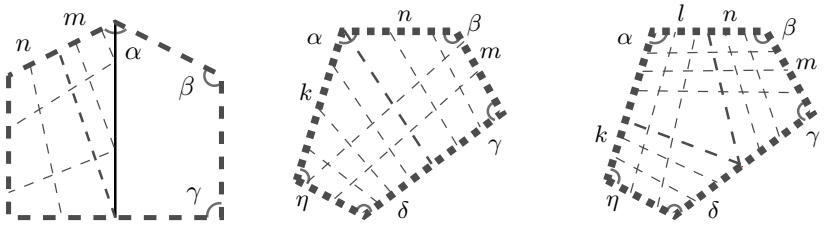

(a) Symmetric pentagon. (b) General pentagon.

Figure 25: Boundary conditions and combinatorics of asymptotic lines for symmetric and general pentagons.

The general case is more difficult. In principle, there are two possibilities for the combinatorial position of an additional umbilic point; see Figure 25(b). The integer parameters correspond to lengths of boundary segments.

4.7.3 A cubical frame

As a last example consider a more complicated polygonal boundary frame as illustrated in Figure 27(a). By construction, the minimal surface spanned by this frame has two planes of reflection symmetry and yet two planar curvature lines. A fundamental piece is therefore bounded by three straight asymptotic lines and two curvature line. Its image under the Gauss map is a spherical triangle with three right angles.

The possible combinatorics of curvature lines are depicted in Figure 27(b). The three integer parameters correspond to the three edge lengths of the cuboid. A minimal surface constructed by this boundary conditions is shown in Figure 26 (left) and can be continued across the boundary to result in a triply periodic minimal surface. Of course, this example may be generalized to related problems. Figure 26 (right) shows an example of such a generalization.

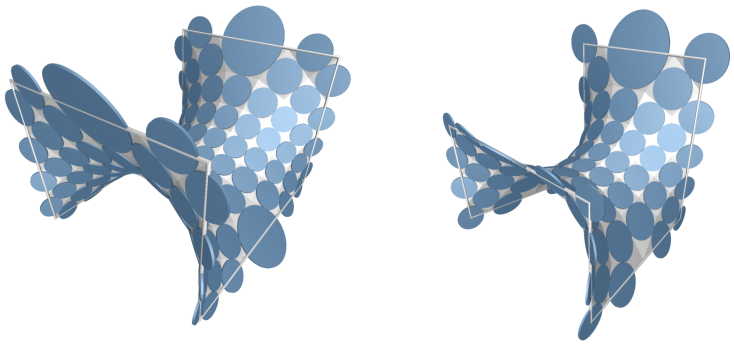

Figure 26: An example of a discrete minimal surface with cubical boundary frame (left, first case of Figure 27(b) with $k = 2, n = 4$) and a generalization (right).

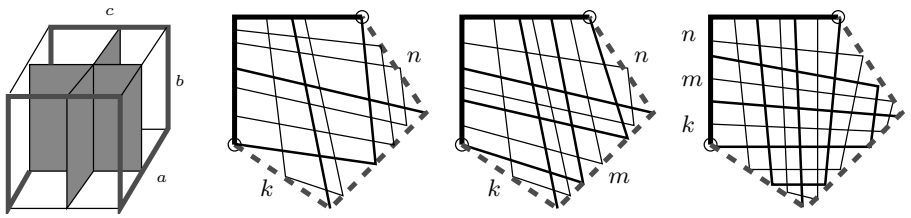

(a) A cubic boundary frame and its symmetry planes.

(b) Different possible types for the combinatorics of curvature lines of a fundamental piece.

Figure 27: A general cubical boundary frame.

5 Weierstrass representation and convergence of discrete minimal surfaces

The convergence of the S-isothermic discrete minimal surfaces can easily be deduced from the convergence of the orthogonal circle patterns, which are used for the construction of the associated Koebe polyhedron, to the corresponding smooth Gauss map. More precisely, we prove the convergence of the stereographic projections of the spherical orthogonal circle patterns to the corresponding complex Gauss map. Then the convergence of the corresponding S-isothermic discrete minimal surfaces is obtained using a suitable discrete Weierstrass respresentation.

5.1 Discrete Weierstrass representation

The classical Weierstrass representation relates a conformal mapping of the complex plane, i.e. a bijective holomorphic mapping, to a smooth minimal surface. In the discrete case, we take suitable orthogonal circle patterns with the same combinatorics as discrete conformal mappings. This leads to an analogous discrete Weierstrass representation formula.

Theorem 5.1 (Discrete Weierstrass representation; [1, Theorem 6])**.** *Let $\mathscr{D}$ be an S-quad-graph. Let $\mathscr{C}$ be a planar orthogonal circle pattern for $\mathscr{D}$. Denote the centers and intersection points of this circle pattern by $c_{\mathscr{C}}$ and $p_{\mathscr{C}}$ respectively. Then an S-isothermic discrete minimal surface $F : V(\mathscr{D}_{\textcircled{s}}) \to \mathbb{R}^3$ is given by the following formula:*

Let $v_1, v_2 \in V(\mathscr{D}_{\textcircled{s}})$ be two vertices, which correspond to touching circles of the pattern. Let $y \in V_b(\mathscr{D})$ be the black vertex between v_1 and v_2, which corresponds to the point of contact. Then the centers $F(v_1)$ and $F(v_2)$ of the corresponding touching spheres of the S-isothermic discrete minimal surface F satisfy

$$F(v_2) - F(v_1) = \pm Re\left(\frac{r(v_2)+r(v_1)}{1+|p|^2}\frac{\overline{c_{\mathscr{C}}(v_2)-c_{\mathscr{C}}(v_1)}}{|c_{\mathscr{C}}(v_2)-c_{\mathscr{C}}(v_1)|}\begin{pmatrix}1-p^2\\ i(1+p^2)\\ 2p\end{pmatrix}\right), \quad (7)$$

where $p = p_{\mathscr{C}}(y)$ and the radii $r(v_j)$ of the spheres are

$$r(v_j) = \left|\frac{1+|c_{\mathscr{C}}(x_j)|^2-|c_{\mathscr{C}}(x_j)p|^2}{2|c_{\mathscr{C}}(x_j)-p|}\right|. \quad (8)$$

The sign on the right-hand side of equation (7) *depends on the label of the edge connecting v_1 with v_2.*

5.2 Convergence of discrete minimal surfaces

The discrete Weierstrass representation and its smooth analogon are the basis of our convergence proof. In fact, note that C^∞-convergence of the orthogonal circle patterns to a conformal mapping implies the C^∞-convergence of the associated discrete S-isothermic minimal surfaces (suitably scaled and translated) to the corresponding smooth minimal surface.

We restrict ourselves to the class of (discrete) minimal surfaces which are bounded, homeomorphic to a disk, and have a boundary curve consisting of planar curvature lines or straight asymptotic lines. As a simple example, consider a part of Schwarz's D surface.

First, we fix some notation. Let SGD be the regular square grid cell decomposition of the complex plane, that is the vertices are $V(SGD) = \mathbb{Z} + i\mathbb{Z}$ and the edges are given by pairs of vertices $[z, z']$ with $z, z' \in V(SGD)$ and $|z - z'| = 1$. Bicolor the vertices $V(SGD)$ such that the black vertices are $V_b(SGD) = \{n + im \in \mathbb{Z} + i\mathbb{Z} : n + m = 1 \pmod 2\}$ and the white vertices are $V_w(SGD) = \{n + im \in \mathbb{Z} + i\mathbb{Z} : n + m = 0 \pmod 2\}$.

Adding circles of radius 1 with centers at the vertices $V_b(SGD)$ leads to an isoradial circle pattern filling the whole complex plane, where circles intersect only orthogonally or touch.

Definition 5.2. Consider a cell decomposition of a two-dimensional manifold which is isomorphic to a subset of SGD and let G be its bicolored graph. An *SG-circle pattern* with the combinatorics of G is a configuration of circles, such that to each white vertex of G there corresponds a circle (all with the same orientation). If two vertices are incident to the same face then the corresponding circles intersect orthogonally. Furthermore, if two vertices are incident to the same black vertex of G but are not incident to the same face, the corresponding circles touch and have disjoint interiors.

Let $\mathcal{D}$ be simply connected bounded region in the complex plane whose boundary is a convex kite with straight edges, or a stereographic projection of a convex spherical kite whose edges are parts of great circles and lying strictly within one half-sphere. Let $\mathcal{R} = \{x + iy : x, y \in [0, 1]\}$ be the closed unit square in $\mathbb{R}^2 \cong \mathbb{C}$.

For $n \in \mathbb{N}$, denote by SG_n the cell decomposition SGD scaled by the factor $1/(2n) > 0$. Denote the subdecomposition corresponding to all vertices of SG_n contained in $\mathcal{R}$ by $SG_n^{\mathcal{R}}$. By abuse of notation, we will not distinguish between the abstract cell decomposition $SG_n^{\mathcal{R}}$ and its embedding into $\mathcal{R}$. The isoradial orthogonal circle pattern of all circles with the same radius $1/(2n)$ and centers in the white vertices $V_w(SG_n^{\mathcal{R}})$ is denoted by $\mathscr{C}_n$. The four vertices $a + ib \in V_w(SG_n^{\mathcal{R}})$ with $a, b \in \{0, 1\}$ at the corners of $\mathcal{R}$ will be referred to as *corner points* of $\mathcal{R}$.

Assume that for each $n \in \mathbb{N}$ there is an SG-circle pattern $\mathscr{C}_n^{\mathcal{D}}$ with the combinatorics of $SG_n^{\mathcal{R}}$ such that all boundary circles intersect the boundary $\partial\mathcal{D}$ orthogonally and the circles corresponding to corner points of $SG_n^{\mathcal{R}}$ intersect the two corresponding boundary arcs of $\partial\mathcal{D}$ orthogonally. In the case of a convex kite (i.e. straight edges), the existence of $\mathscr{C}_n^{\mathcal{D}}$ is guaranteed by Theorem 3.4. The general question on existence for the spherical case is still open, see Section 3 and [1] for further remarks and special cases. Nevertheless, existence can be proven for some special cases, for example for a symmetric spherical quadrilateral with angles $\alpha = 2\pi/3 = \gamma$, $\beta = \pi/2 = \delta$. This choice of angles leads to four fundamental pieces of Schwarz's D surface bounded by four planar curvature lines, see Section 4.3.

Given the cell decomposition $SG_n^{\mathcal{R}}$, we can easily obtain a triangulation by adding edges between white vertices which are incident to the same face. Given the circle patterns $\mathscr{C}_n$ and $\mathscr{C}_n^{\mathcal{D}}$, we denote the embeddings of the above triangulations by $T_n \subset \mathcal{R}$ and $T_n^{\mathcal{D}} \subset \mathcal{D}_n$ respectively. Here $\mathcal{D}_n$ is the convex hull of the centers and the intersection points of $\mathscr{C}_n^{\mathcal{D}}$. Note that all triangles of T_n and $T_n^{\mathcal{D}}$ are right-angled. Now we construct a homeomorphism corresponding to the circle patterns which approximates a given conformal mapping from $\mathcal{R}$ onto $\mathcal{D}$.

Fix a conformal homeomorphism from $\mathcal{R}$ onto $\mathcal{D}$ which maps the corner points of $\mathcal{R}$ to the corner points of $\mathcal{D}$. Let g^{corn} be the restriction of g to the corner points of $\mathcal{R}$. Denote by g_n^{corn} the corresponding bijective mapping which maps the corner points of $\mathcal{R}$ to the corresponding centers of circles of $\mathscr{C}_n^{\mathcal{D}}$. As approximating mapping we define $g_n : \mathcal{R} \to \mathcal{D}_n$ to be the simplicial map determined by the correspondence of vertices and edges of T_n and $T_n^{\mathcal{D}}$ which agrees with g_n^{corn} at the corner points. Recall that a simplicial map for two triangulations as T_n and $T_n^{\mathcal{D}}$ maps vertices to corresponding vertices and is linear on every triangular face. An example of $\mathscr{C}_n$ and $\mathscr{C}_n^{\mathcal{D}}$ – and hence g_n – is given in Figure 28.

For abbreviation we denote $\mathcal{R}^* = \mathcal{R} \backslash \{\text{corner points}\}$. Compact sets $K \subset \mathcal{R}^*$ will always mean compact subsets of $\mathbb{C}$ with respect to the standard metric which are contained in $\mathcal{R}^*$. Furthermore, we define the radius function $r_n : V_w(SG_n^{\mathcal{R}}) \to (0, \infty)$ of $\mathscr{C}_n^{\mathcal{D}}$ which assigns to every white vertex the radius of the corresponding circle of $\mathscr{C}_n^{\mathcal{D}}$. Now we can state our convergence result:

Theorem 5.3. *The mappings g_n converge to the unique conformal homeomorphism $g : \mathcal{R} \to \mathcal{D}$ which coincides with g^{corn} at the corner points. The con-*

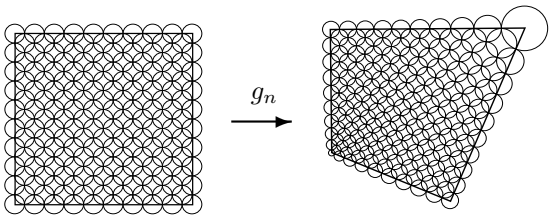

Figure 28: An example of two corresponding orthogonal circle patterns filling a square and a kite-shaped convex quadrilateral respectively.

vergence is uniform on $\mathcal{R}$ and in C^∞ on compact subsets of $\mathcal{R}^*$. Furthermore, the quotients of corresponding radii, $2nr_n$, converge to $|g'|$ in C^∞ uniformly on compact subsets of $\mathcal{R}^*$.

A detailed version and a generalization of Theorem 5.3 as well as a proof can be found in [10, Chapter 7] or in [11].

Remark 5.4. If the angle of $\mathcal{D}$ at a corner point is $\pi/2$ then the convergence is also in C^∞ on compact sets of $\mathcal{R}$ including the corresponding corner point.

Instead of $\mathcal{R}$, we may consider the rotated region $\mathcal{R}' = \mathrm{e}^{i\pi/4}\mathcal{R}$ and the part of SG_n contained in $\mathcal{R}'$. Note that the corresponding combinatorics differ from $SG_n^{\mathcal{R}}$. Theorem 5.3 also holds in this case.

Theorem 5.5. *Let $\mathcal{D}$ be the projection of a symmetric spherical quadrilateral $Q \subset \mathbb{S}^2$ bounded by parts of great circles which is entirely contained in one half of the sphere. Assume that for all $n \in \mathbb{N}$ orthogonal circle pattens $\mathscr{C}_n^{\mathcal{D}}$ with the combinatorics of $SG_n^{\mathcal{R}}$ exist such that all boundary circles intersect the boundary $\partial\mathcal{D}$ orthogonally and the circles corresponding to corner points of $SG_n^{\mathcal{R}}$ intersect two corresponding boundary lines of $\partial\mathcal{D}$ orthogonally. For $n \in \mathbb{N}$, define g_n as in Theorem 5.3.*

Let F_n be the discrete minimal surface obtained from the stereographic projection of $\mathscr{C}_n^{\mathcal{D}}$ by dualization and scaled as in Theorem 5.1. Then the scaled S-isothermic discrete minimal surfaces M_n corresponding to $\frac{1}{n^2}F_n$ converge uniformly for the images of compact subsets of $\mathcal{R}^*$ to a smooth minimal surface M. The stereographic projection of the Gauss map, determining M up to translation and scaling, is given by the conformal map $g : \mathcal{R} \to \mathcal{D}$.

The proof is a straight forward application of the Weierstrass Representation Theorem 5.1, see also the proof of [1, Theorem 9].

References

[1] A. I. Bobenko, T. Hoffmann, and B. A. Springborn, *Minimal surfaces from circle patterns: Geometry from combinatorics*, Ann. of Math. **164** (2006), no. 1, 231–264.

[2] A. I. Bobenko and U. Pinkall, *Discrete isothermic surfaces*, J. reine angew. Math. **475** (1996), 187–208.

[3] ———, *Discretization of surfaces and integrable systems*, Discrete Integrable Geometry and Physics (A. I. Bobenko and R. Seiler, eds.), Clarendon Press, 1999, pp. 3–58.

[4] A. I. Bobenko, H. Pottmann, and J. Wallner, *A curvature theory for discrete surfaces based on mesh parallelity*, Math. Annalen **348** (2010), 1–24.

[5] A. I. Bobenko and B. A. Springborn, *Variational principles for circle patterns and Koebe's theorem*, Trans. Amer. Math. Soc. **356** (2004), 659–689.

[6] ———, *A discrete Laplace-Beltrami operator for simplicial surfaces*, Discr. Comp. Geom. **38** (2007), 740–756.

[7] A. I. Bobenko and Yu. B. Suris, *Discrete Differential Geometry. Integrable Structure*, Graduate Studies in Mathematics, vol. 98, AMS, 2008.

[8] K. A. Brakke, *Triply periodic minimal surfaces*, Internet, cited 2014 Apr 25, `http://www.susqu.edu/facstaff/b/brakke/evolver/examples/periodic/periodic.html`.

[9] G. R. Brightwell and E. R. Scheinerman, *Representations of planar graphs*, SIAM J. Discr. Math. **6** (1993), no. 2, 214–229.

[10] U. Bücking, *Approximation of conformal mappings by circle patterns and discrete minimal surfaces*, Ph.D. thesis, Technische Universität Berlin, 2007, published online at `http://opus.kobv.de/tuberlin/volltexte/2008/1764/`.

[11] ———, *Approximation of conformal mappings by circle patterns*, Geom. Dedicata **137** (2008), 163–197.

[12] E.-B. Christoffel, *über einige allgemeine Eigenschaften der Minimumsflächen*, J. Reine Angew. Math. **67** (1867), 218–228.

[13] P. G. Ciarlet, *The finite element method for elliptic problems*, Studies in mathematics and its applications, North-Holland, Amsterdam, 1978.

[14] U. Dierkes, S. Hildebrandt, A. Küster, and O. Wohlrab, *Minimal Surfaces I*, Springer-Verlag, Berlin, 1992.

[15] G. Dziuk, *An algorithm for evolutionary surfaces*, Numer. Math. **58** (1991), 603–611.

[16] G. Dziuk and J. E. Hutchinson, *The discrete Plateau problem: Algorithm and numerics*, Math. Comp. **68** (1999), no. 225, 1–23.

[17] J. D. Gergonne, *Questions proposées/résolues*, Ann. Math. Pure Appl. **7** (1816), 68, 99–100, 156, 143–147.

[18] Udo Hertrich-Jeromin, *Introduction to Möbius differential geometry*, London Mathematical Society Lecture Note Series, vol. 300, Cambridge University Press, 2003.

[19] H. Karcher, *The triply periodic minimal surfaces of Alan Schoen and their constant mean curvature companions*, Manuscr. Math. **64** (1989), 291–357.

[20] P. Koebe, *Kontaktprobleme der konformen Abbildung*, Abh. Sächs. Akad. Wiss. Leipzig Math.-Natur. Kl. **88** (1936), 141–164.

[21] Ch. Müller and J. Wallner, *Oriented mixed area and discrete minimal surfaces*, Discrete Comput. Geom. **43** (2010), 303–320.

[22] E. R. Neovius, *Bestimmung zweier spezieller periodischer Minimalflächen, auf welchen unendlich viele gerade Linien und unendlich viele ebene geodätische Linien liegen*, J. C. Frenckell & Sohn, Helsingfors, 1883.

[23] J. C. C. Nitsche, *Lectures on minimal surfaces,* vol. 1, Cambridge University Press, 1989.

[24] U. Pinkall and K. Polthier, *Computing discrete minimal surfaces and their conjugates*, Exp. Math. **2** (1993), 15–36.

[25] Helmut Pottmann, Yang Liu, Johannes Wallner, Alexander Bobenko, and Wenping Wang, *Geometry of multi-layer freeform structures for architecture*, ACM Trans. Graphics **26** (2007), no. 3, Proc. SIGGRAPH.

[26] B. Riemann, *Über die Fläche vom kleinsten Inhalt bei gegebener Begrenzung*, Abh. Königl. Ges. d. Wiss. Göttingen, Mathem. Cl. **13** (1867), 3–52, K. Hattendorff, edit.

[27] ———, *Gesammelte Mathematische Werke*, B.G. Teubner, 1876 (1st ed.), 1892 (2nd ed.), and additions 1902.

[28] I. Rivin, *A characterization of ideal polyhedra in hyperbolic 3-space*, Ann. of Math. **143** (1996), 51–70.

[29] R. Schneider, *Convex bodies: the Brunn-Minkowski theory*, Cambridge University Press, 1993.

[30] A. H. Schoen, *Infinte periodic minimal surfaces without self-intersections*, NASA Technical Note (1970), no. D-5541.

[31] O. Schramm, *How to cage an egg*, Invent. Math. **107** (1992), no. 3, 543–560.

[32] H. A. Schwarz, *Gesammelte Mathematische Abhandlungen,* vol. 1, Springer-Verlag, Berlin, 1890.

[33] Stefan Sechelmann, *Discrete Minimal Surfaces, Koebe Polyhedra, and Alexandrov's Theorem. Variational Principles, Algorithms, and Implementation.*, Diploma thesis, Technische Universität Berlin, 2007.

[34] B. A. Springborn, *Variational principles for circle patterns*, Ph.D. thesis, Technische Universität Berlin, 2003, published online at `http://opus.kobv.de/tuberlin/volltexte/2003/668/`.

[35] T. Tsuchiya, *Discrete solution of the Plateau problem and its convergence*, Math. Comp. **49** (1987), 157–165.